Atmos. Chem. Phys. Discuss., 13, 31013–31040, 2013
www.atmos-chem-phys-discuss.net/13/31013/2013/
doi:10.5194/acpd-13-31013-2013

Atmospheric Chemistry and Physics Discussions

Snow cover sensitivity to black carbon deposition in the Himalaya: from atmospheric and ice core measurements to regional climate simulations

M. Ménégoz[1,2], G. Krinner[1,2], Y. Balkanski[3], O. Boucher[4], A. Cozic[3], S. Lim[1,2], P. Ginot[1,2,5], P. Laj[1,2], H. W. Jacobi[1,2], H. Gallée[1,2], and A. Marinoni[6,7]

[1]Laboratoire de Glaciologie et GéCNRS Grenoble 1 Géophysique de l'Environnement (LGGE, UMR5183), 38041 Grenoble, France
[2]UJF Grenoble 1, Laboratoire de Glaciologie et Géophysique de l'Environnement (LGGE, UMR5183), 38041 Grenoble, France
[3]Laboratoire des Sciences du Climat et de l'Environnement, IPSL, CEA-CNRS-UVSQ, Gif-sur-Yvette, France
[4]Laboratoire de Mé téorologie Dynamique, IPSL, CNRS, Paris, France
[5]IRD/UJF – Grenoble 1/CNRS/U. Savoie/INPG/IFSTTAR/CNRM, Observatoire des Sciences de l'Univers de Grenoble (OSUG) UMS222, Grenoble, 38041, France
[6]CNR-ISAC-Institute of Atmospheric Sciences and Climate, Bologna, Italy
[7]EV-K2-CNR Committee, Bergamo, Italy

Received: 23 October 2013 – Accepted: 11 November 2013 – Published: 27 November 2013
Correspondence to: M. Ménégoz (martin.menegoz@lgge.obs.ujf-grenoble.fr)
Published by Copernicus Publications on behalf of the European Geosciences Union.

ACPD
13, 31013–31040, 2013

Abstract

We applied a climate-chemistry model to evaluate the impact of black carbon (BC) deposition on the Himalayan snow cover from 1998 to 2008. Using a stretched grid with a resolution of 50 km over this complex topography, the model reproduces reasonably well the observations of both the snow cover duration and the seasonal cycle of the atmospheric BC concentration including a maximum in atmospheric BC during the pre-monsoon period. Comparing the simulated BC concentrations in the snow with observations is challenging because of the high spatial variability and the complex vertical distribution of BC in the snow. We estimate that both wet and dry BC depositions affect the Himalayan snow cover reducing its annual duration by one to eight days. The resulting increase of the net shortwave radiation at the surface reaches an annual mean of 1 to 3 $W m^{-2}$, leading to a localised warming of 0.05 to 0.3 °C.

1 Introduction

Black carbon (BC) is one of the main anthropogenic pollutants affecting the climate system. Bond et al. (2013) estimated the total climate forcing of BC through all forcing mechanisms to be about +1.1 $W m^{-2}$ with a 90 % probability to be included in a range of +0.17 to +2.1 $W m^{-2}$. This value includes the net effect of BC on radiation and clouds, but also that on snow albedo, which has been found to strongly impact the climate system (Hansen and Nazarenko, 2004). Anthropogenic BC deposited on snow was found to shorten by several days the current duration of the snow cover season in the Northern Hemisphere (Ménégoz et al., 2013a) and to contribute to the significant decrease of the snow cover extent observed during the last decades (Dery et al., 2007). Brutel-Vuilmet et al., (2013) found the new generation of global climate model to simulate correctly the present-day snow cover extent, but to underestimate its decrease over the last decades. They also noted that coarse-gridded models simulate particularly badly the snow cover over mountainous areas.

ACPD
13, 31013–31040, 2013

The Himalayan region hosts extended glaciers (Kääb et al., 2012). Wide areas of North western and Eastern Himalaya are snow covered during a large fraction of the year, whereas in central Himalaya the snow cover extent is rather limited (Ménégoz et al., 2013b). The Himalayan atmosphere is strongly affected by anthropogenic emissions of BC originating from the Indian plain and highly populated mountainous areas (Ohara et al., 2007). Consequently, atmospheric BC can reach very high concentrations (Ramanathan et al., 2007) even at high altitude (Bonasoni et al., 2010; Kopacz et al., 2011; Marinoni et al., 2013). Ice cores drilled in this region have shown that aerosol pollution is incorporated into the snowpack even at very high altitude (e.g., Ming et al., 2008, 2009; Xu et al., 2009; Ginot et al., 2013). Yasunari et al. (2010, 2013) estimated that BC in snow reduces its albedo on average by 5 % at the southern slopes of the Nepalese Himalaya. Kopacz et al. (2011) found the radiative forcing due to BC on snow to vary from 5 to 15 $\mathrm{W\,m^{-2}}$ within the snow-covered areas of this region, while Flanner et al. (2007) estimated peak values of 20 $\mathrm{W\,m^{-2}}$ for some parts of the Tibetan Plateau. Menon et al. (2010) proposed that during the last decade BC in snow caused a significant part of the decrease of the snow cover extent observed in this region.

Since these last modelling studies have been based on relatively coarse-gridded models, their ability to simulate the snow cover over mountainous areas remained relatively limited. Here, we use a global climate model with a stretched grid, to reach a fine resolution over the Himalaya, in order to quantify the effect of BC deposition on the snow cover duration. The temporal variation and magnitude of the aerosol concentration both in the atmosphere and snow are compared to observations. Finally, we estimate the snow cover duration, surface radiation, and temperature changes induced by the BC deposition on Himalayan snow.

ACPD
13, 31013–31040, 2013

2 Experimental setup

2.1 The LMDZ-ORCHIDEE-INCA climate model

We used the LMDZ-ORCHIDEE-INCA atmospheric general circulation model to study the interactions between the atmosphere, aerosols, and snow-covered areas in the Himalaya. This model consists of three coupled modules. The LMDZ general circulation model represents the atmospheric component (Hourdin et al., 2006). The ORCHIDEE land surface model describes exchanges of energy and water between the atmosphere, the soil and the biosphere (Krinner et al., 2005) and includes a dynamic snow module. The coupling between LMDz and ORCHIDEE is described in Hourdin et al. (2006). INCA (interactions between chemistry and aerosols) describes gas- and aqueous-phase chemistry (Hauglustaine et al., 2004) as well as aerosol physical properties such as size and hygroscopicity (Balkanski et al., 2010), which control the amount of wet and dry deposition. The coupling of LMDZ and INCA detailed in Szopa et al. (2013) allows an interactive simulation of five aerosol chemical species: Sulphate, BC, organic carbon (OC), sea salt, and dust. We consider aerosol-radiation interactions for BC, OC, sea salt, and dust and aerosol-cloud interactions for sulphate, BC, and OC as described in Déandreis et al. (2012). Here, we used the detailed representation of snow cover implemented in ORCHIDEE by Krinner et al. (2006) and used in Ménégoz et al. (2013a). This includes a two-layer scheme that describes the snow albedo as a function of snow grain size and aerosol content in the snow based on Wiscombe and Warren (1980). The representation of snow grain size and BC in the snow and the snow albedo scheme implemented in our model are detailed in Ménégoz et al. (2013a). Since we want our simulation to be in phase with the atmospheric observations, in particular with the East Asian and the Indian monsoons that bring a large amount of moisture in the Himalaya, all simulations were performed with winds nudged toward the ECMWF ERA-interim reanalysis: Each 150 s (5 times the time step with that wind velocities are computed), horizontal wind velocities are nudged at all altitudes with a relaxation time of 1 h over the Himalayan region and 30 min elsewhere. Hence, the

ACPD
13, 31013–31040, 2013

model is very constrained by the reanalysis outside the Himalayan region, whereas it evolves more independently inside (see details in Coindreau et al., 2007).

2.2 Resolution of the simulation

We performed simulations for the 1998–2008 period with two different grids: a first one with a regular coarse horizontal resolution (96 × 95 grid points corresponding to ∼ 350 km), and a second one with a 143 × 144 stretched grid with a zoom on the Himalaya reaching a 50 km resolution over this region. Comparisons with satellite observations (see Fig. 1) show that a fine resolution is essential to simulate correctly the observed snow cover duration over the Hindu Kush Himalaya region and the Tibetan Plateau: the coarse-gridded simulation (Fig. 1a) shows a strong overestimation of the snow cover duration, in particular over the Tibetan Plateau, in comparison with satellite observations interpolated onto the same grid (Fig. 1c). Interpolating the output of the simulation based on the stretched grid onto the coarse grid (Fig. 1b), we see that this bias is strongly reduced. Such an improvement is due to a better representation of the local atmospheric circulation and climate feedbacks using a fine resolution. The simulation based on the stretched grid is quite similar to the satellite observation (Fig. 1d and e) with high values of snow cover duration in the high mountains of the Hindu Kush Himalaya and large parts of the Tibetan Plateau free of snow most of the year. Note, however, that the overestimation of the snow cover duration over the Tibetan Plateau does not fully disappear when increasing the resolution of the model. In the following, we focus only on simulations performed with the stretched grid, which appears essential to describe snow cover variations in the Himalaya.

ACPD
13, 31013–31040, 2013

3 Aerosol deposition on snow

3.1 Model vs. observations of atmospheric BC

As part of the international exercise AEROCOM (see http://aerocom.met.no/Welcome.html), Koch et al. (2009) analysed the capabilities of global aerosol models to simulate BC. Like most other models, INCA has been found to generally underestimate the aerosol absorption optical depth. A different behaviour was found for the modelled BC surface concentration, which is generally overestimated in Europe and underestimated in Asia. In particular, INCA using a coarse grid (96 × 95 grid points, i.e. ∼ 350 km) was found to underestimate by a factor of two on average the surface concentrations over entire Asia. Only sparse observational data are available in the Himalayan region (Nair et al., 2013) making it difficult to evaluate the performance of global aerosol models in this region. To our knowledge, such models have only been validated in terms of aerosol deposition on snow in these areas (e.g. Kopackz et al., 2011).

To investigate the ability of our model to describe the atmospheric concentration of aerosol in high altitude areas of the Himalaya, we use here observations performed since 2006 at the Nepal Climate Observatory-Pyramid (NCO-P, 27.95° N, 86.82° E, 5079 m a.s.l., Bonasoni et al., 2010), in the region of Mount Everest. At NCO-P, BC is observed using a Multi-Angle Absorption Photometer (MAAP) providing measurement of aerosol absorption coefficient that can be converted to Equivalent Black Carbon (EBC, Petzold et al., 2005). In the following, MAAP-derived EBC will be labelled BC for simplifying reading of the paper although we are well aware of denomination recommendations from Petzold et al. (2013). Table 1 shows observed and modelled atmospheric concentrations of BC at this site considering the year-dependant seasons as defined in Bonasoni et al. (2008). The order of magnitude and the annual cycle of the observed BC concentration are relatively well reproduced by our model with minimum values occurring during the monsoon, higher values during the winter, and maximum values before and after the monsoon. However, the simulated BC maximum occurs in the post-monsoon period, whereas it is observed during the pre-monsoon period.

ACPD
13, 31013–31040, 2013

The maximum daily average value observed from 2006 to 2007 reaches 2500 ng m^{-3} whereas the simulated BC never exceeds 550 ng m^{-3} during the same period. Such observed high values may be due to a thermally-driven atmospheric circulation that cannot be represented in a model at 50 km horizontal resolution.

3.2 Model vs. observations of BC deposited on snow

Simulated aerosol deposition and aerosol concentration in the snow are now compared to the information recorded in a shallow ice core extracted from the Mera Glacier (6376 m a.s.l, 27.7° N, 86.9° E, Nepal), a high altitude site located 35 km south from the NCO-P site. This ice core was used to reconstruct both the evolution and the deposition flux of several proxies including BC and dust over the period 1998–2008 (Ginot et al., 2013). This 19.8 m core was sub-sampled with a mean resolution of 6.6 cm. Note that BC is in that case determined using a Single Particle Soot Photometer (SP2) and corresponds to refractory BC (rBC) according to the recommendation from Petzold et al., 2013. Lim et al. (2013) compared EC (from thermo-optical techniques) to rBC (SP2) in Himalayan snow. Overall, the EC/rBC is >1 and often close to 3. This has to be accounted for in the comparisons, as we expect our BC simulations to be closer to EC than rBC observations, since they were performed with IPCC emission inventories mainly based on emission factors derived from thermal-optical methods (Lamarque et al., 2012; Petzold et al., 2013). In the following, we compare these ice core observations with our simulation focusing on BC and dust concentrations in the snow and their deposition fluxes. We do not expect our coarse-gridded model to reproduce the local BC observations in the snow, but we test if our model is able to reproduce the temporal variation of BC observed in snow. We use also this comparison to evaluate the order of magnitude of BC in snow. The altitude of the model grid cell containing the Mera Glacier is too low to simulate a continuous seasonal snow cover in winter/spring. Therefore, we used for our comparison a grid cell located 50 km further north at an altitude high enough (5552 m a.s.l.) to conserve a continuous seasonal snow cover in the

ACPD
13, 31013–31040, 2013

simulations. Here, the monsoon period is defined as JJAS, pre- and post-monsoon as AM and ON, and winter as DJFM. Due to strong winds eroding the snow at the surface (Wagnon et al., 2013), the winter deposition fluxes could not be provided from the ice core (except for the last year of the period 1998–2008) and we grouped winter, pre- and post-monsoon into one period designed as inter-monsoon period.

Observed and simulated BC concentrations in the snow are reported in Table 2. Very large discrepancies exist between modelled and observed BC concentrations in the snow: the modelled annual mean value (201 $\mu g\,kg^{-1}$) is 60 times higher than the mean observed value (3.0 $\mu g\,kg^{-1}$). Monsoon and inter-monsoon modelled values (285 and 28 $\mu g\,kg^{-1}$, respectively) are 30 times higher than the observed values (9.2 and 1.0 $\mu g\,kg^{-1}$, respectively). Note the winter difference is also very high (not shown because observed values are available only for a part of the winter 2008, the winter snow of the previous years was totally eroded by strong local winds), which explains the seasonal differences to be lower than the annual mean difference. Even with a difference of more than one order of magnitude, the modelled and observed BC concentrations in the snow show a similar seasonal cycle, with inter-monsoon values ten times larger than the monsoon values. Modelled annual BC deposition flux is 16 times higher than the flux deduced from the ice core (model: 53 $mg\,m^{-2}\,yr^{-1}$, observation: 3.2 $mg\,m^{-2}\,yr^{-1}$). Both in the model and in the ice core, the inter-monsoon period is characterised by high levels of BC deposition (model: 58 %, observation: 75 %), whereas this flux is lower during the monsoon period (model: 42 %, observation 25 %).

Modelled dust concentration in the snow reaches 10.4 $mg\,kg^{-1}$, close to the value observed in the ice core (10.1 $mg\,kg^{-1}$). Measurements of dust concentrations do not show any seasonal cycle, whereas simulated concentrations are two times lower during the monsoon (5 $mg\,kg^{-1}$). Modelled and observed dust depositions are similar with an annual mean of 10.1 $g\,m^{-2}\,yr^{-1}$ in the ice core and 6.4 $g\,m^{-2}\,yr^{-1}$ in our simulation. However, observed dust deposition is three times larger during the monsoon, which is in contrast to our simulation with a flux slightly lower during the monsoon compared to the inter-monsoon flux. This may be due to a compensating effect since Ginot et al.,

ACPD
13, 31013–31040, 2013

(2013) showed that a large fraction of dust is emitted locally, a small scale process that is not represented in our coarse-gridded model.

Note that we simulated an annual mean of snowfall that reaches 83 mm w.eq. yr^{-1} on the model grid cell used for our comparison. At the ice core drilling site, snowfall has not been measured, but Ginot et al. (2013) report an annual mean of snow accumulation of 94 mm w.eq. yr^{-1}. The observed annual snow accumulation results from the snowfall lowered by sublimation, melting and wind erosion (Wagnon et al., 2013), and cannot be directly compared with our modelled snowfall. Moreover, we cannot expect our model to simulate accurately the local snow accumulation since it remains relatively coarse-gridded even with a stretched grid. The similarity of order of magnitude of the observed snow accumulation and the modelled snowfall is clearly a coincidence. Still, it indicates that the difference between modelled and observed concentration of aerosol in the snow, particularly marked for BC, cannot be explained by a difference in snow accumulation.

3.3 How to explain the differences between simulations and observations?

Comparing large-scale outputs of a global climate model with local observations is challenging, in particular over a complex topography area, where models are not able to describe the high spatial variability of the atmospheric circulation and surface processes. Even it can appear hazardous to compare BC in snow modelled with a two-layers snow scheme at a resolution of 50 km with local observations. Still, such comparison is essential to check the capabilities of climate models, and to analyses physical processes that involve global to local scales. In the following, we show five points that can explain the differences between our simulations and available observational data:

1. Due to its resolution, the grid cell of the model used here for comparison with the observations has an average altitude of 5552 m a.s.l., approximately 1000 m lower than the site where the ice core was drilled. Since we simulated a strong vertical gradient of the BC concentration in the atmosphere (not shown), the modelled

ACPD
13, 31013–31040, 2013

rates of BC are more characteristic of the Himalayan valleys than high summits areas, less polluted since they reach the altitude of the free troposphere (Bonasoni et al., 2008). Lim et al. (2013) determined the BC concentration in snow sampled close to the NCO-P observatory (5079 m a.s.l). They measured an rBC concentration ranging from 2 to 23 $\mu g\,kg^{-1}$, and an EC concentration between 6 and 57 $\mu g\,kg^{-1}$. Such values, higher than those measured in the Mera Peak ice core indicate that the Himalayan snow is more polluted at lower altitudes than at high altitudes. Regarding the ice core of the Mera Glacier, the higher concentration of dust in comparison with that of BC suggests that dust is transported in the atmosphere via high altitude pathways in contrast to BC that stays in the lower layers of the atmosphere. Similarly in the Himalayan region, Fadnavis et al. (2013) estimated from aerosol simulations and satellite observations that dust concentration reaches high and relatively homogeneous concentration below 6500 m (i.e. under ~ 500 hPa). According to their study, the vertical gradient of BC in the atmosphere below 6500 m appears to be more pronounced for BC than for dust. Such a difference can explain that our model reproduces well the dust concentration in the snow observed at the Mera Glacier whereas it gives higher values for BC in comparison with the observation because the altitude of the used model grid cell is 1000 m below the ice core drilling site.

2. The BC concentration shows large vertical variations trough the snowpack (Ming et al., 2009). The estimate of the BC surface concentration in the snow strongly depends on the snow thickness considered when analysing both observations and model outputs. In the model the surface snow layer corresponds to the top 8 mm snow water equivalent (SWE, see Ménégoz et al., 2013a) of the snowpack, whereas the vertical resolution of the Mera Glacier ice core is 6.6 cm SWE. Since most of the BC deposited is accumulated in the top layer of the model, considering a thicker top layer in our simulation would result in lower concentrations: as an example, with a concentration of BC in the bottom snow layer equal to zero and considering a depth of 8 cm instead of 8 mm for the top layer corresponds

ACPD
13, 31013–31040, 2013

to a reduction of the surface concentration by a factor of 10. Ming et al. (2009) considered a 1 m depth for the surface snow layer, for which they found a BC concentration of 18 $\mu g\,kg^{-1}$ for the East Rongbuk Glacier making it difficult to compare with our modelled value. In addition, the question about a possible flushing of BC particles trough snow layers is still unresolved: performing observations at 2000 m a.s.l. in the Northern United Stated under particularly high rates of snow melting, Conway et al. (1996) observed a diffusion of BC particles trough the snow layers. Similar experiments performed in Spitsbergen by Aamaas et al. (2011) led to a contrary conclusion based on the observations that BC tends to stay at the surface of the snowpack even during melting conditions. We concluded that we couldn't implement a parameterisation describing such processes in our model due to the strong lack of observations. Still, we considered in our model that all the deposited BC stays at the surface as long as there is no snowfall without any flushing of particles trough the snow layers (Ménégoz et al., 2013a). This assumption could overestimate both the BC concentration in the top snow layer and the magnitude of the BC effects on the snow cover and the climate. It can also partially explain why the ratio between modelled and observed BC concentrations in the snow is larger than that for the deposition fluxes (60 vs. 16, see Table 2). However, this assumption does not impact the modelled flux of BC deposited at the surface modifying only its vertical distribution within the snowpack.

3. The strong winds observed at the drilling site erode unknown amounts of both snow and aerosol in particular during the winter (Wagnon et al., 2013; Ginot et al., 2013). This process is not simulated in our model.

4. Measurements of BC concentrations, both in the atmosphere and in the snow, differ widely according to the method used to perform the observations (Petzold et al., 2013). Overall, different methodologies can lead to differences in BC up to a factor of 5 as reported by Lim et al. (2013). The differences between model

ACPD
13, 31013–31040, 2013

and observations are however too high to be explained only by the difference in measuring techniques.

5. BC deposition strongly varies both spatially and temporally. In an ice core from the East Rongbuk Glacier (28.03° N, 86.96° E, 6518 m a.s.l. Everest region) Kaspari et al. (2011) measured average rBC concentration in snow of 7 $\mu g\,kg^{-1}$ for the recent period using an SP2. They estimated the seasonal mean of rBC concentration in snow to reach a maximum close to 10 $\mu g\,kg^{-1}$ during winter or spring and a background value during the monsoon around 0.1 $\mu g\,kg^{-1}$. These values are similar to those measured at the Mera Peak (see Table 2). Some kilometres farther at the Repula Col (28.02° N, 86.96° E, 6500 m a.s.l.) Ming et al. (2008) found a mean concentration of EC in snow around 20 $\mu g\,kg^{-1}$ using a thermo-optical technique with an opposite seasonal cycle compared to the seasonal cycle observed by Kaspari et al. (2011). In their observations, the maximal concentration of EC in snow occurs during the monsoon with values sometimes exceeding 50 $\mu g\,kg^{-1}$. Kaspari et al. (2011) estimated the dry deposition to be the main sinks of atmospheric BC in the Everest region, whereas Ming et al. (2008) estimated BC to be incorporated in snow mainly by wet deposition. In a further study, Ming et al. (2009) measured the BC concentration in the snow of different mountainous areas in Western China. On the South of the Tibetan Plateau, they measured vertical profiles of BC in snow with a resolution of 5 cm finding concentrations ranging between 22 and 600 $\mu g\,kg^{-1}$ closer to our modelled values. Modelled results are similar to highest BC mixing ratios derived by thermo-optical methods. As explained previously, emission factors used in inventories made for climate models are often derived from EC measurements. Therefore, a comparison with thermo-optical methods may be more appropriate than a comparison with SP2-derived values. Nevertheless, it is clear that individual measurement sites may not be representative of a model grid-box.

ACPD
13, 31013–31040, 2013

3.4 Estimating wet and dry aerosol deposition in the Himalaya

We now examine the relative importance of wet vs. dry deposition of BC in Himalaya. We simulate high amounts of BC and dust wet deposition in the region of the Mera Glacier because dry deposition represents locally only 11 % of the simulated total deposition (Table 2). Many previous published studies have focused only on the role of dry deposition of BC on the snow albedo in the Himalaya. As an example, Yasunari et al. (2010, 2013) estimated dry deposition velocities and corresponding snow albedo variations at the NCO-P site. They forced their simulations with the atmospheric measurements of Bonasoni et al. (2010), who pointed out the high spring atmospheric BC concentration. Yasunari et al. (2010, 2013) estimated the BC deposition from March to May 2006 to reach 900–1300 $\mu g\,m^{-2}$ inducing a concentration of BC in snow ranging between 26 to 68 $\mu g\,kg^{-1}$. Considering only dry deposition in our simulations leads to a similar deposition flux (480 $\mu g\,m^{-2}$ for the same period) and to an equivalent BC concentration in snow of 43 $\mu g\,kg^{-1}$. However, the model indicates that large amounts of BC in snow originate from wet deposition, both during monsoon and inter-monsoon period. We suggest, therefore, that the maximum of BC observed in the Mera ice core is largely due to wet deposition and not only to dry deposition as often suggested (Yasunari et al., 2010, 2013). This assumption is reinforced by Ming et al. (2008, 2009) who found that the BC concentration in snow reaches a maximum during the monsoon period, exceeding values of 50 $\mu g\,kg^{-1}$. Reconstructing the atmospheric concentration of BC, they considered that most of the BC in the ice core originated from wet deposition. In our simulation, dry deposition reaches strong values during the inter-monsoon period at the southern slopes of the Himalaya (Fig. 2a). During this dry period, simulated wet deposition plays a minor role over the Indian subcontinent, but there is still some precipitation in particular over the Western and the Eastern part of the Himalaya inducing a large amount of wet deposition in these regions (Fig. 2b). During the monsoon simulated dry deposition is weaker than during the inter-monsoon period (Fig. 2c). During the same period, due to high precipitation rates, wet deposition is enhanced over the

ACPD
13, 31013–31040, 2013

entire Indian subcontinent (Fig. 2d), in particular in the Indo-Gangetic Plain, where very high amounts of BC are emitted (not shown). The atmospheric residence time of BC (i.e. the ratio between the atmospheric BC concentration and the BC deposition rate) is, therefore, limited, but still long enough to allow a significant transport of BC towards the Himalaya in our simulation leading to large wet deposition rates over the Hindu Kush Himalaya region and the Tibetan Plateau. Finally, we assume that the diminution of the atmospheric BC concentration observed at the NCO-P observatory is not due to a reduction of the aerosol transport from polluted areas in the south, but rather to a decrease of the atmospheric residence time of BC. Even with significant amounts of BC deposited on snow during the monsoon, the BC concentration in snow decreases as snowfall occurring at the same time strongly dilutes the aerosol concentration in the snow. The pronounced spatial heterogeneity of precipitation in the Himalaya (Ménégoz et al., 2013b) may induce large spatial variations of BC wet deposition, which certainly explains most of the difference between the observations of BC in snow performed by Ginot et al. (2013), Ming et al. (2008) and Kaspari et al. (2011). There is a strong need for more observations to quantify accurately both the BC wet deposition and the BC concentration in the snow at different altitudes. Still, our model and most of the observations show BC in snow to reach a maximum in spring, a period of the year characterized by an increase of both dry and wet BC deposition concomitant with low levels of snowfall and increasing levels of sublimation and melting. In the absence of flushing, all these factors enhance the BC concentration at the surface of the snow cover. In our 1998–2008 simulation, the spring maximum concentration of BC in the surface snow layer (i.e. the upper 8 mm SWE) reaches spatially highly variable values ranging from 50 to 500 $\mu g\,kg^{-1}$ (Fig. 3a).

4 BC deposition impact on snow cover and surface energy balance

To quantify the effect of BC deposition on Himalayan snow, denominated here as the "snow darkening effect" (Bond et al., 2013), we performed two simulations with and

ACPD
13, 31013–31040, 2013

without BC in snow. Note that the atmospheric effects of BC are taken into account in both simulations. We diagnosed the modifications induced by the forcing of BC deposited on snow including the so-called "rapid adjustments" (IPCC, 2013), but only parts of longer-timescale feedbacks since the winds were nudged toward the reanalysis of the ECMWF in our simulation (see Sect. 2.1). In parts of Nepal, the annual mean of snow cover duration is reduced by two to five days (Fig. 3b). However, due to the relatively small surface covered by seasonal snow in Nepal, this decrease remains limited to a small area. In contrast, larger areas in the Karakoram, and in the Western and the Eastern Himalaya experience a decrease of one to eight days per year of the snow cover duration due to the snow darkening effect. These variations are statistically significant at a 95 % level according to a two-sample *t* test. The simulated annual mean of snow cover duration is quite low over the Tibetan Plateau (Fig. 1d). Therefore, its sensitivity to aerosol deposition remains limited, and we modelled no significant variation of the snow cover duration in this region. We assume that previous studies based on coarse-gridded models (e.g., Flanner et al., 2007; Menon et al., 2010) strongly overestimate the forcing of BC in the Tibetan Plateau. Such overestimation is not due to a bad representation of the BC forcing itself, but rather to an overestimation of the snow cover extent in this region, which cannot be well simulated with a coarse resolution model.

In the regions where the BC deposition on snow induces a decrease of the snow cover duration, we found a positive increase in net surface solar radiation that varied between 1 and 3 $W m^{-2}$ on average for 1998 to 2008 (Fig. 3c). This surface net radiative forcing is of the same order of magnitude as previous local estimates. Based on a simple radiative model transfer, Ginot et al. (2013) found the BC measured in their ice core to increase the net surface radiative balance by 2 $W m^{-2}$. Similarly, Ming et al. (2008) reported a mean surface forcing for the BC deposited on snow of 1 to 1.5 $W m^{-2}$ at the end of the 20th century and Kaspari et al. (2011) calculated a forcing of 0.5 $W m^{-2}$ over the last decades. The surface radiative forcing estimated in our study is necessarily higher as these last studies because it takes also into account rapid adjustments (in particular the faster growth of the snow grain size if the snow

ACPD
13, 31013–31040, 2013

becomes warmer in the presence of BC). In addition, the number of days when the surface albedo has values corresponding to snow-free surfaces instead of values of snowy surfaces is increased when BC in the snow is taken into account for the snow albedo computation. The forcing estimated in Fig. 3c includes also this excess of solar energy absorbed by the surface when it is free of snow. Finally, the surface forcing of BC in snow that we estimated here includes the BC particles itself with all the rapid adjustments, but excludes parts of slow feedbacks that are associated with modifications of the atmospheric circulation, the hydrological cycle, and changes in sea surface temperature. Further sensitivities studies may be performed with our model to evaluate separately these processes as done by Menon et al. (2010) with a coarse-gridded GCM. In our simulation, the BC deposition on snow results in an increase of the mean surface temperature over 1998–2008 ranging from 0.05 to 0.3 °C (Fig. 3d). This temperature modification is statistically significant according to a two-sample t test (not shown). It consists in an upper estimation because we modelled BC concentrations in the snow that can be realistic, but that were found elevated in comparison with the observations.

5 Conclusions

We applied a coupled climate-chemistry model to evaluate the impact of BC deposition on snow cover in the Himalayas from 1998 to 2008 through snow albedo variations. When compared to satellite observations, the snow cover simulated with coarse-gridded models appears particularly biased by the absence of the representation of the complex topography. Simulating atmospheric circulation and surface energy balance with a finer resolution allows a more realistic representation of the snow cover duration. Our model reproduces the seasonal variations of the atmospheric BC concentrations observed in the Mount Everest region with maximum values occurring in the pre-monsoon period. Estimating the BC concentration in snow is more difficult due to the high spatial variability of dry and wet deposition and to the complex vertical

ACPD
13, 31013–31040, 2013

distribution of BC in the snowpack. Our model simulates a BC dry deposition flux in accordance with previous local analysis. However, we purport that wet deposition brings also large amounts of BC to the Himalayan snow. This wet deposition does not increase directly the concentration of BC in the snow, in particular during the monsoon, because snowfall also brings fresh snow at the surface that is cleaner than the old surface layer, highly concentrated in BC. However, it plays a significant role in reducing the snow albedo: when periods of sunny days occur after snowfall events, melting and sublimation dramatically concentrate BC at the surface. Such events likely occur in spring during the progressive onset of the monsoon (Molg et al., 2012) and occasionally in summer. Then, the atmosphere is quickly cleaned by higher rates of wet deposition causing significant levels of BC in the snow. More observations are needed to estimate the actual rates of BC wet deposition in this region. In addition, field campaigns dedicated to observe the vertical profile of BC in the snowpack are helpful to improve our understanding of the snow darkening effect. Finally, we estimate here the BC deposited to the snow to decrease the snow cover duration by one to eight days per year in the mountains of the Hindu Kush Himalaya with a seasonal snow cover. We found this anthropogenic forcing to have a limited impact on the snow cover of the Tibetan Plateau, a dry region only partially snow covered, even during the monsoon-accumulation period. Considering the BC forcing with rapid adjustments, part of the slow feedbacks, and in particular the removal of snow during some days per year, we found the surface of mountainous region of the Himalaya to absorb an excess of 1 to 3 $W m^{-2}$. This forcing cannot be considered as representative of glaciated areas since these are never free of snow except for debris-covered glaciers. Further simulations considering a permanent snow cover on current glaciated areas could be used to simulate the forcing of BC over glaciers. Finally, we estimate the BC deposition on Himalayan snow to increase the annual mean temperature by 0.05 to 0.3 °C between 1998 and 2008.

Acknowledgements. This work was supported by the Agence Nationale de la Recherche under contract ANR-09-CEP-005-02/PAPRIKA. We thank the "Commissariat à l'Energie Atomique et aux Energies Alternatives" and GENCI for providing computer time for the simulations

ACPD
13, 31013–31040, 2013

presented in this paper. The figures have been prepared with Ferret free software. We thank the National Snow and Ice Data Centre (NSIDC, Boulder, CO) for providing IMS daily Northern Hemisphere snow and ice analysis. We thank Patrick Wagnon, Adrien Gilbert, and Yves Arnaud for the ice core they extracted from the Mera Glacier, and Patrick Wagnon and Etienne Berthier for their useful comments on the manuscript.

The publication of this article is financed by CNRS-INSU.

References

Balkanski, Y., Myhre, G., Gauss, M., Rädel, G., Highwood, E. J., and Shine, K. P.: Direct radiative effect of aerosols emitted by transport: from road, shipping and aviation, Atmos. Chem. Phys., 10, 4477–4489, doi:10.5194/acp-10-4477-2010, 2010.

Bonasoni, P., Laj, P., Marinoni, A., Sprenger, M., Angelini, F., Arduini, J., Bonafè, U., Calzolari, F., Colombo, T., Decesari, S., Di Biagio, C., di Sarra, A. G., Evangelisti, F., Duchi, R., Facchini, MC., Fuzzi, S., Gobbi, G. P., Maione, M., Panday, A., Roccato, F., Sellegri, K., Venzac, H., Verza, GP., Villani, P., Vuillermoz, E., and Cristofanelli, P.: Atmospheric Brown Clouds in the Himalayas: first two years of continuous observations at the Nepal Climate Observatory-Pyramid (5079 m), Atmos. Chem. Phys., 10, 7515–7531, doi:10.5194/acp-10-7515-2010, 2010.

Bond, T. C., Doherty, S. J., Fahey, D. W., Forster, P. M., Berntsen, T., De Angelo, B. J., Flanner, M.G., Ghan, S., Karcher, B., Koch, D., Kinne, S., Kondo, Y., Quinn, P. K., Sarofim, M. C., Schultz, M. G., Schulz, M., Venkataraman, C., Zhang, H., Zhang, S., Bellouin, N., Guttikunda, S. K., Hopke, P. K., Jacob- son, M. Z., Kaiser, J. W., Klimont, Z., Lohmann, U., Schwarz, J. P., Shindell, D., Storelvmo, T., Warren, S. G., and Zender, C. S.: Bounding the role of black carbon in the climate system: a scientific assessment, J. Geophys. Res. Atmos., 118, 5380–5552, doi:10.1002/jgrd.50171, 2013

ACPD
13, 31013–31040, 2013

Brutel-Vuilmet, C., Ménégoz, M., and Krinner, G.: An analysis of present and future seasonal Northern Hemisphere land snow cover simulated by CMIP5 coupled climate models, The Cryosphere, 7, 67–80, doi:10.5194/tc-7-67-2013, 2013.

Coindreau, O., Hourdin, F., Haeffelin, M., Mathieu, A., and Rio, C.: Assessment of physical parameterizations using a global climate model with stretchable grid and nudging, Mon. Weather Rev., 135, 1474–1489, 2007.

Déandreis, C., Balkanski, Y., Dufresne, J. L., and Cozic, A.: Radiative forcing estimates of sulfate aerosol in coupled climate-chemistry models with emphasis on the role of the temporal variability, Atmos. Chem. Phys., 12, 5583–5602, doi:10.5194/acp-12-5583-2012, 2012.

Déry, S. J. and Brown, R. D.: Recent Northern Hemisphere snow cover extent trends and implications for the snow-albedo feedback, Geophys. Res. Lett., 34, L22504, doi:10.1029/2007GL031474, 2007.

Fadnavis, S., Semeniuk, K., Pozzoli, L., Schultz, M. G., Ghude, S. D., Das, S., and Kakatkar, R.: Transport of aerosols into the UTLS and their impact on the Asian monsoon region as seen in a global model simulation, Atmos. Chem. Phys., 13, 8771–8786, doi:10.5194/acp-13-8771-2013, 2013.

Flanner, M. G., Zender, C. S., Randerson, J. T., and Rasch, P. J.: Present-day climate forcing and response from black carbon in snow, J. Geophys. Res., 112, D11202, doi:10.1029/2006JD008003, 2007.

Ginot, P., Dumont, M., Lim, S., Patris, N., Taupin, J.-D., Wagnon, P., Arnaud, Y., and Laj. P.: Black carbon and dust impact on Himalayan glacier melting simulated from Mera Peak ice core record (Nepal), submitted, 2013.

Hansen, J. and Nazarenko, L.: Soot climate forcing via snow and ice albedos, P. Natl. Acad. Sci. USA, 101, 423–428, doi:10.1073/pnas2237157100, 2004.

Hauglustaine, D. A., Hourdin, F., Jourdain, L., Filiberti, M. A., Walters, S., Lamarque, J. F., and Holland, E. A.: Interactive chemistry in the Laboratoire de Météorologie Dynamique general circulation model: description and background tropospheric chemistry evaluation, J. Geophys. Res., 109, D04314, doi:10.1029/2003JD003957, 2004.

Hourdin. F., Musat, I., Bony, S., Braconnot, P., Codron, F., Dufresne, J.-L., Fairhead, L., Filiberti, M.-A., Friedlingstein, P., Grandpeix, J.-Y., Krinner, G., LeVan, P., Li, Z.-X., and Lott, F.: The LMDZ4 general circulation model: Climate performance and sensitivity to parametrized physics with emphasis on tropical convection, Clim. Dynam., 27, 787–813, 2006.

ACPD
13, 31013–31040, 2013

IPCC: Climate Change 2013: The Physical Science Basis, Contribution of Working Group I to the Fourth Assessment, Report of the Intergovernmental Panel on Climate Change, in press, 2013.

Kääb, A., Berthier, E., Nuth, C., Gardelle, J., and Arnaud, Y.: Contrasting patterns of early 21st century glacier mass change in the Himalaya, Nature, 488, 495–498, doi:10.1038/nature11324, 2012.

Kaspari, S. D., Schwikowski, M., Gysel, M., Flanner, M. G., Kang, S., Hou, S., and Mayewski, P. A.: Recent increase in black carbon concentrations from a Mt. Everest ice core spanning 1860–2000 AD, Geophys. Res. Lett., 38, L04703, doi:10.1029/2010GL046096, 2011.

Koch, D., Schulz, M., Kinne, S., McNaughton, C., Spackman, J. R., Balkanski, Y., Bauer, S., Berntsen, T., Bond, T. C., Boucher, O., Chin, M., Clarke, A., De Luca, N., Dentener, F., Diehl, T., Dubovik, O., Easter, R., Fahey, D. W., Feichter, J., Fillmore, D., Freitag, S., Ghan, S., Ginoux, P., Gong, S., Horowitz, L., Iversen, T., Kirkevåg, A., Klimont, Z., Kondo, Y., Krol, M., Liu, X., Miller, R., Montanaro, V., Moteki, N., Myhre, G., Penner, J. E., Perlwitz, J., Pitari, G., Reddy, S., Sahu, L., Sakamoto, H., Schuster, G., Schwarz, J. P., Seland, Ø., Stier, P., Takegawa, N., Takemura, T., Textor, C., van Aardenne, J. A., and Zhao, Y.: Evaluation of black carbon estimations in global aerosol models, Atmos. Chem. Phys., 9, 9001–9026, doi:10.5194/acp-9-9001-2009, 2009.

Kopacz, M., Mauzerall, D. L., Wang, J., Leibensperger, E. M., Henze, D. K., and Singh, K.: Origin and radiative forcing of black carbon transported to the Himalayas and Tibetan Plateau, Atmos. Chem. Phys., 11, 2837–2852, doi:10.5194/acp-11-2837-2011, 2011.

Krinner, G., Boucher, O., and Balkanski, Y.: Ice-free glacial northern Asia due to dust deposition on snow, Clim. Dynam., 27, 613– 625, 2006.

Lamarque, J.-F., Granier, C., Bond, T., Eyrling, V., Heil, A., Kainuma, M., Lee, D., Liousse, C., Mieville, A., Riahi, K., Schultz, M., Sith, S., Stehfest, E., Stevenson, D., Thomson, A., vanAardenne, J., and vanVuuren, D.: Gridded emissions in sup- port of IPCC AR5, IGAC Newsl., 41, 12–18, 2009.

Lim, S., Cozic, J., Faïn, X., Zanatta, M., Jaffrezo, J.-L., Ginot, P., and Laj, P.: Optimizing measurement methodology of refractory black carbon concentration in snow and ice and intercomparison with EC measurement method, submitted, 2013.

Marinoni, A., Cristofanelli, P., Laj, P., Duchi, R., Putero, D., Calzolari, F., Landi, T. C., Vuillermoz, E., Maione, M., Bonasoni, P., High black carbon and ozone concentrations during pol-

ACPD
13, 31013–31040, 2013

lution transport in the Himalayas: five years of continuous observations at NCO-P global GAW station, J. Environ. Sci., 25, 1618–1625, doi:10.1016/S1001-0742(12)60242-3, 2013.
Ménégoz, M., Krinner, G., Balkanski, Y., Cozic, A., Boucher, O., and Ciais, P.: Boreal and temperate snow cover variations induced by black carbon emissions in the middle of the 21st century, The Cryosphere, 7, 537–554, doi:10.5194/tc-7-537-2013, 2013a.
Ménégoz, M., Gallée, H., and Jacobi, H. W.: Precipitation and snow cover in the Himalaya: from reanalysis to regional climate simulations, Hydrol. Earth Syst. Sci., 17, 3921–3936, doi:10.5194/hess-17-3921-2013, 2013b.
Menon, S., Koch, D., Beig, G., Sahu, S., Fasullo, J., and Orlikowski, D.: Black carbon aerosols and the third polar ice cap, Atmos. Chem. Phys., 10, 4559–4571, doi:10.5194/acp-10-4559-2010, 2010.
Ming, J., Cachier, H., Xiao, C., Qin, D., Kang, S., Hou, S., and Xu, J.: Black carbon record based on a shallow Himalayan ice core and its climatic implications, Atmos. Chem. Phys., 8, 1343–1352, doi:10.5194/acp-8-1343-2008, 2008.
Ming, J., Xiao, C., Cachier, H., Qin, D., Qin, X., Li, Z., and Pu, J.: Black Carbon (BC) in the snow of glaciers in west China and its potential effects on albedos, Atmos. Res., 92, 114–123, 2009.
Mölg, T., Maussion, F., Yang, W., and Scherer, D.: The footprint of Asian monsoon dynamics in the mass and energy balance of a Tibetan glacier, The Cryosphere, 6, 1445–1461, doi:10.5194/tc-6-1445-2012, 2012.
Nair, V. S., Babu, S. S., Moorthy, K. K., Sharma, A. K., and Marinoni, A.: Black carbon aerosols over the Himalayas: direct and surface albedo forcing, Tellus B, 65, 19738, doi:10.3402/tellusb.v65i0.19738, 2013.
National Ice Center, updated daily. IMS Daily Northern Hemisphere Snow and Ice Analysis at 4 km and 24 km Resolution. Boulder, Colorado USA: National Snow and Ice Data Center, digital media, doi:10.7265/N52R3PMC, 2008.
Ohara, T., Akimoto, H., Kurokawa, J., Horii, N., Yamaji, K., Yan, X., and Hayasaka, T.: An Asian emission inventory of anthropogenic emission sources for the period 1980–2020, Atmos. Chem. Phys., 7, 4419–4444, doi:10.5194/acp-7-4419-2007, 2007.
Petzold, A., Schloesser, H., Sheridan, P. J., Arnott, W. P., Ogren, J. A., and Virkkula, A.: Evaluation of multiangle absorption photometry for measuring aerosol light absorption, Aerosol Sci. Tech., 39, 40–51, 2005.

ACPD
13, 31013–31040, 2013

Petzold, A., Ogren, J. A., Fiebig, M., Laj, P., Li, S.-M., Baltensperger, U., Holzer-Popp, T., Kinne, S., Pappalardo, G., Sugimoto, N., Wehrli, C., Wiedensohler, A., and Zhang, X.-Y.: Recommendations for reporting "black carbon" measurements, Atmos. Chem. Phys., 13, 8365–8379, doi:10.5194/acp-13-8365-2013, 2013.

Ramanathan, V., Li, F., Ramana, M. V., Praveen, P. S., Kim, D., Corrigan, C. E., Nguyen, H., Stone, E. A., Schauer, J. J., Carmichael, G. R., Adhikary, B., and Yoon, S. C.: Atmospheric brown clouds: Hemispherical and regional variations in long-range transport, absorption, and radiative forcing, J. Geophys. Res., 112, D22S21, doi:10.1029/2006JD008124, 2007.

Szopa, S., Balkanski, Y., Schulz, M., Bekki, S., Cugnet, D., Fortems-Cheiney, A., Turquety, S., Cozic, A., Déandreis, C., Hauglustaine, D., Idelkadi, A., Lathière, J., Lefevre, F., Marchand, M., Vuolo, R., Yan, N., and Dufresne, J.-L.: Aerosol and ozone changes as forcing for climate evolution between 1850 and 2100, Clim. Dynam., 40, 1–28, doi:10.1007/s00382-012-1408-y, 2013.

Xu, B., Cao, J., Hansen, J., Yao, T., Joswia, D. R., Wang, N., and He, J.: Black soot and the survival of Tibetan glaciers, P. Natl. Acad. Sci. USA, 106, 22114–22118, 2009.

Yasunari, T. J., Bonasoni, P., Laj, P., Fujita, K., Vuillermoz, E., Marinoni, A., Cristofanelli, P., Duchi, R., Tartari, G., and Lau, K.-M.: Estimated impact of black carbon deposition during pre-monsoon season from Nepal Climate Observatory – Pyramid data and snow albedo changes over Himalayan glaciers, Atmos. Chem. Phys., 10, 6603–6615, doi:10.5194/acp-10-6603-2010, 2010.

Yasunari, T. J., Tian, Q., Lau, K. M., Bonasoni, P., Marinoni, A., Laj, P., Ménégoz, M., Takemura, T., and Chin, M., Estimated range of black carbon dry deposition and the related snow albedo reduction over Himalayan glaciers during dry pre-monsoon periods, Atmos. Environ., 78, 259–267, doi:10.1016/j.atmosenv.2012.03.031, 2013.

Wagnon, P., Vincent, C., Arnaud, Y., Berthier, E., Vuillermoz, E., Gruber, S., Ménégoz, M., Gilbert, A., Dumont, M., Shea, J. M., Stumm, D., and Pokhrel, B. K.: Seasonal and annual mass balances of Mera and Pokalde glaciers (Nepal Himalaya) since 2007, The Cryosphere, 7, 1769–1786, doi:10.5194/tc-7-1769-2013, 2013.

Wiscombe, W. and Warren, S.: A model for the spectral albedo of snow, II: Snow containing atmospheric aerosols, J. Atmos. Sci., 37, 2734–2745, 1980.

ACPD
13, 31013–31040, 2013

Table 1. Summary of atmospheric concentrations of BC observed at the Nepal Climate Observatory-Pyramid (NCO-P, 27.95° N, 86.82° E, 5079 m a.s.l., from March 2006 to February 2008, Bonasoni et al., 2010) and modelled with LMDZ-INCA. The corresponding grid cell of the model is located at 4480 m a.s.l. and seasons are defined as in Table 1 of Bonasoni et al. (2010).

[BC] (ng m^{-3})	Pre-monsoon	Monsoon	Post- monsoon	Winter	Maximum
Observations	316	50	135	119	2500
Model	206	76	224	138	550

ACPD
13, 31013–31040, 2013

Table 2. BC and dust concentration in the snow, and BC and dust deposition reconstructed from an ice core drilled at 27.7° N, 86.9° E, 6376 m a.s.l. (Ginot et al., 2013); all percentages are computed from the annual values. The model grid cell is located 50 km northward, where the altitude of the model surface is high enough to allow a continuous seasonal snow cover (28.0° N, 86.9° E, 5552 m a.s.l). Ginot et al. (2013) computed the annual mean aerosol concentration by multiplying the seasonal snow accumulation by the seasonal aerosol concentration. For the entire period 1998–2008, they used the winter concentration of the last year, since it was the only one available, the others being eroded by winds. Inter-monsoon modelled concentrations include winter values. Annual modelled values are the temporal average of the aerosol concentration in the top snow layer of the model (i.e. a constant surface depth of 8 mm snow water).

		Annual	Inter-monsoon	Monsoon
BC concentration ($\mu g\,kg^{-1}$)	Observation	3.0	9.2	1.0
	Model	201	285	28
BC deposition ($mg\,m^{-2}\,yr^{-1}$)	Observation	3.2	75 %	25 %
	Model	53 (11 % dry)	58 % (8 % dry; 50 % wet)	42 % (3 % dry, 39 % wet)
Dust concentration ($mg\,kg^{-1}$)	Observation	10.1	11.1	10.1
	Model	10.4	13	5
Dust deposition ($g\,m^{-2}\,yr^{-1}$)	Observation	10.1	28 %	72 %
	Model	6.4 (10 % dry)	60 % (6 % dry, 54 % wet)	40 % (4 % dry, 36 % wet)

ACPD
13, 31013–31040, 2013

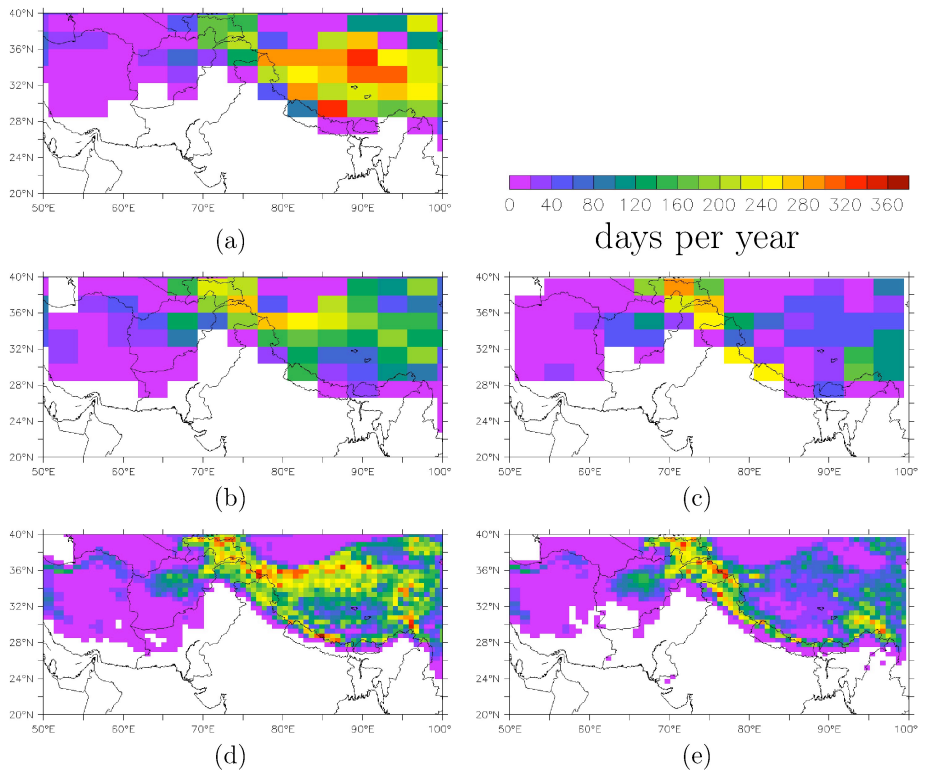

Fig. 1. Annual mean snow cover duration, days per year) averaged over 1998–2008: **(a)** LMDZ coarse-gridded simulation (~ 350 km). **(b)** LMDZ simulation based on a stretched grid (~ 50 km) interpolated on the coarse grid of LMDZ. **(c)** Satellite observation interpolated on the coarse grid of LMDZ. **(d)** LMDZ simulation based on a stretched grid (~ 50 km). **(e)** Satellite observation interpolated on the LMDZ stretched grid. LMDZ simulations were performed with the BC effect on snow albedo. IMS satellite observations are from NSIDC (2008).

ACPD
13, 31013–31040, 2013

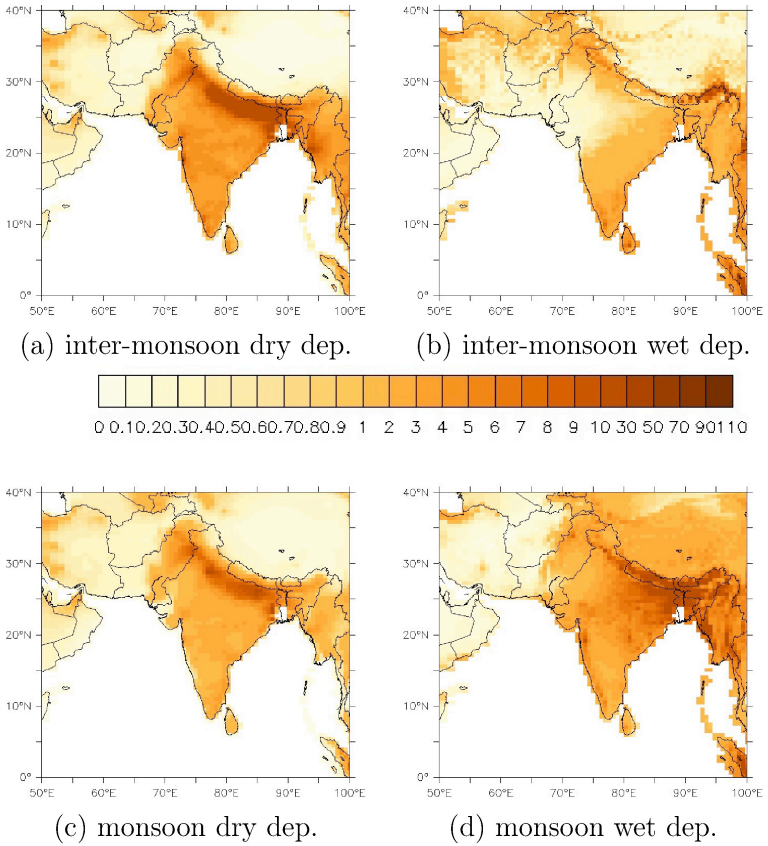

Fig. 2. BC deposition ($mg\,m^{-2}\,month^{-1}$) modelled over the Indian subcontinent averaged over 1998–2008. **(a)** Inter-monsoon (ONDJFMAM) dry-deposited BC. **(b)** Inter-monsoon wet-deposited BC. **(c)** Monsoon (JJAS) dry-deposited BC. **(d)** Monsoon wet-deposited BC. LMDZ simulation based on a stretched grid reaching a resolution of ~ 50 km over the Himalaya.

ACPD
13, 31013–31040, 2013

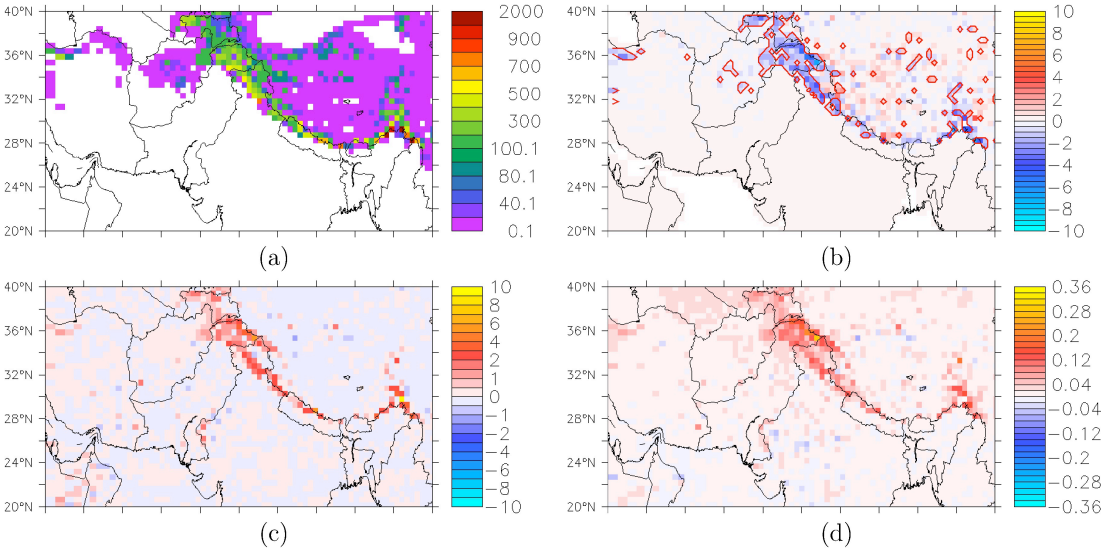

Fig. 3. (a) Simulated spring BC mixing ratio ($\mu g\,kg^{-1}$) in the surface snow layer (8 mm SWE). **(b)** Difference in annual mean of snow cover duration (days per year) between two simulations performed with and without the snow albedo variations induced by BC deposition. Areas with statistically significant differences, according to a two-sample *t* test, are red-contoured. **(c)** Same difference but for annual mean net surface solar radiation ($W\,m^{-2}$). **(d)** Same difference but for annual mean temperature (°C). LMDZ simulation are based on a stretched grid reaching a resolution of ~ 50 km over the Himalaya.

ACPD
13, 31013–31040, 2013